as a function of the free-energy change for reductive and oxidative quenching (eq 2 and 3). It can be seen that the points which correspond to the quenching mechanism that is thought to be the most probable on the basis of the above discussion lie on a Marcus-type "band".[19] The scattering of these points from a common curve is not unexpected, because the excited states, and even more so the quenchers, differ in their inherent barriers to electron transfer.[27] It is noteworthy that in the cases for which an energy-transfer mechanism has been thought to be the most probable, both of the points corresponding to the electron-transfer mechanisms lie far from the Marcus-type curve.

Acknowledgment. The authors are grateful to Professors V. Balzani and L. Moggi for their interest in this work and for their helpful criticism. Financial support from the National Research Council of Italy and from the European Communities (Contract No. 031-76ESI) is appreciated.

Registry No. $Cr(bpy)_3^{3+}$, 15276-15-0; $Ru(bpy)_3^{2+}$, 15158-62-0; $Os(bpy)_3^{2+}$, 23648-06-8; $Mo(CN)_8^{4-}$, 17923-49-8; $Cr(CN)_6^{3-}$, 14875-14-0; $Fe(CN)_6^{4-}$, 13408-63-4; $Fe(CN)_6^{3-}$, 13408-62-3; $Ru(CN)_6^{4-}$, 21029-33-4; $Co(CN)_6^{3-}$, 14897-04-2; $Ni(CN)_4^{2-}$, 15453-80-2.

References and Notes

(1) On leave from the Department of Chemistry, Concordia University, Montreal, Québec, Canada.
(2) V. Balzani, L. Moggi, M. F. Manfrin, F. Bolletta, and G. S. Laurence, *Coord. Chem. Rev.*, **15**, 321 (1975).
(3) V. L. Ermolaev, E. G. Sveshnikova, and T. A. Shakhverdov, *Russ. Chem. Rev.* (*Engl. Transl.*), **44**, 26 (1975).
(4) C.-T. Lin, W. Böttcher, M. Chou, C. Creutz, and N. Sutin, *J. Am. Chem. Soc.*, **98**, 6536 (1976), and references cited therein.
(5) A. R. Gutierrez, T. J. Meyer, and D. G. Whitten, *Mol. Photochem.*, **7**, 349 (1976), and references cited therein.
(6) R. Ballardini, G. Varani, F. Scandola, and V. Balzani, *J. Am. Chem. Soc.*, **98**, 7432 (1976), and references cited therein.
(7) C. Creutz and N. Sutin, *Proc. Natl. Acad. Sci. U.S.A.*, **72**, 2858 (1975).
(8) G. Sprintschnik, M. W. Sprintschnik, P. P. Kirsch, and D. G. Whitten, *J. Am. Chem. Soc.*, **98**, 2337 (1976); **99**, 4947 (1977).
(9) A. Juris, M. T. Gandolfi, M. F. Manfrin, and V. Balzani, *J. Am. Chem. Soc.*, **98**, 1047 (1976).
(10) B. R. Baker and B. D. Mehta, *Inorg. Chem.*, **4**, 848 (1965).
(11) F. H. Burstall, *J. Chem. Soc.*, 173 (1936).
(12) F. H. Burstall, F. P. Dwyer, and E. C. Gyarfas, *J. Chem. Soc.*, 953 (1950).
(13) N. A. P. Kane-Maguire, J. Conway, and C. H. Langford, *J. Chem. Soc., Chem. Commun.*, 801 (1974); I. Fujita and H. Kobayashi, *Z. Phys. Chem.* (*Frankfurt am Main*), **79**, 309 (1972), and references cited therein.
(14) K. König and S. Herzog, *J. Inorg. Nucl. Chem.*, **32**, 585 (1970); G. M. Bryant, J. E. Fergusson, and H. K. J. Powell, *Aust. J. Chem.*, **24**, 257 (1971).
(15) I. B. Berlman, "Handbook of Fluorescence Spectra and Aromatic Molecules", Academic Press, New York, N.Y., 1971.
(16) M. Maestri, F. Bolletta, L. Moggi, V. Balzani, M. S. Henry, and M. Z. Hoffman, *J. Am. Chem. Soc.*, **100**, 2694 (1978).
(17) C.-T. Lin and N. Sutin, *J. Phys. Chem.*, **80**, 97 (1976); C. R. Bock, T. J. Meyer, and D. G. Whitten, *J. Am. Chem. Soc.*, **97**, 2909 (1975).
(18) J. B. Headridge, "Electrochemical Techniques for Inorganic Chemists", Academic Press, New York, N.Y., p 71.
(19) R. A. Marcus, *Annu. Rev. Phys. Chem.*, **15**, 155 (1964).
(20) F. Bolletta, M. Maestri, and V. Balzani, *J. Phys. Chem.*, **80**, 2499 (1976).
(21) F. Wilkinson and A. Farmilo, *J. Chem. Soc., Faraday Trans. 2*, **72**, 604 (1976).
(22) C. Creutz and N. Sutin, *J. Am. Chem. Soc.*, **98**, 6384 (1976).
(23) J. N. Demas and J. W. Addington, *J. Am. Chem. Soc.*, **98**, 5800 (1976).
(24) A. V. Kiss, J. Abraham, and I. Hegedüs, *Z. Anorg. Allg. Chem.*, **244**, 98 (1940).
(25) J. Brigando, *Bull. Soc. Chim. Fr.*, 503 (1957).
(26) J. J. Alexander and H. B. Gray, *J. Am. Chem. Soc.*, **90**, 4260 (1968).
(27) H. E. Toma and C. Creutz, *Inorg. Chem.*, **16**, 545 (1977).

Contribution from the Department of Chemistry, Texas A&M University, College Station, Texas 77843

Stereochemical Activity of s Orbitals

MICHAEL B. HALL

Received November 15, 1977

The dependence of the bond angles of AH_n (n = 2, 3, 4, 5, 6) molecules on various energy parameters are studied by extended Hückel theory (EHT). The results suggest that, contrary to the expectations of the valence shell electron pair repulsion (VSEPR) model, the only important Pauli repulsions in "normal" covalent molecules (four or fewer electron pairs) are those between bond pairs. The driving force for bending in a molecule such as H_2O is due primarily to the relative np–ns energy separation of the central atom in agreement with our previous ab initio calculations. Thus, H_2O bends not because there are lone pair–lone pair or lone pair–bond pair repulsions but because the 2s orbital is lower in energy and the molecule can maximize its occupation only by bending. The np–ns energy separation also controls the degree to which three-center, four-electron (3c-4e) bonds bend toward the two-center, two-electron (2c-2e) bonds in molecules such as ClF_3. In these "hypervalent" molecules the Pauli exclusion principle also contributes to the bending. However, this effect does not arise from lone pair–bond pair repulsions but from bond-pair attractions, i.e., the desire to delocalize the "electron-rich" 3c-4e bond into the "electron poor" 2c-2e bond.

Introduction

In our previous ab initio study of the geometry of H_2O[1] we have shown that the basic tenet of the valence shell electron pair repulsions (VSEPR) model,[2] that the geometry is determined by Pauli repulsion of localized lone pairs, is not viable. Rather, the geometry of H_2O is determined by two competing effects: one, the Pauli repulsions between bond pairs, which tend to increase the bond angle; two, the system's desire to lower the total energy by keeping the more stable oxygen 2s orbital fully occupied, which tends to decrease the bond angle. No Pauli repulsions due to the lone pairs were evident in our analysis. Both of these effects are manifest in extended Hückel theory[3] (EHT) and, as we will show, are the primary reason for its often correct prediction of the geometry.

The exact geometry of any molecule is, of course, a complex balance of forces, and we do not want to suggest that a model as simple as EHT can account for all the subtle effects in the total energy. However, for the gross features of the geometry, EHT appears to incorporate the major effects and has had a long success in describing the major qualitative features of the bonding. Allen and co-workers have studied the relation of EHT to ab initio calculations.[4] An examination of EHT and Walsh diagrams has been presented by Gimarc,[5] and Bartell has compared the results of VSEPR and EHT.[6] However, the dependence of the EHT predictions on parameter choice and how this relates to the qualitative description of the geometry

0020-1669/78/1317-2261$01.00/0

have not been examined in detail.

In this work we will analyze the effect of parameter choice on the predicted bond angles both in terms of delocalized orbitals using Walsh diagrams[7] and in terms of localized contributions to the total energy using Ruedenberg's energy partitioning.[8] The analysis of our results gives further support to our contention that the theoretical basis of the VSEPR model is on weak ground. The energy partitioning scheme of Ruedenberg is particularly helpful in this regard since it partitions the energy into quasiclassical atomic contributions and nonclassical interference contributions. The effects of the Pauli repulsions are manifest in the latter term. Because of the freedom of choosing a variety of energy parameters, EHT offers unparalleled opportunity to study the energetic contributions to the total energy and geometry. Neither VSEPR nor EHT makes explicit use of the electron–electron repulsions, but both make use of the Pauli principle, and for VSEPR it is the primary factor in determining the geometry. Rather than make some assumption that certain interactions dominate the total energy, as is done in VSEPR, we will attempt a complete analysis of all the contributions which affect the total energy and, therefore, the geometry. Particularly informative are the parameter choices for which EHT fails to give the correct geometry.

Theory

Extended Hückel theory begins with a single determinant of molecular orbitals (MO) as the total wave function (a simple orbital product would be equivalent since there are no explicit two-electron operators in the EH Hamiltonian). The MO's are then expanded in a linear combination of atomic orbitals (LCAO).

$$\phi_i^{MO} = \sum_a C_{ia} X_a^{AO} \tag{1}$$

The Hamiltonian takes the form of a sum of effective one-electron operators and the C's are varied to minimize the energy. This reduces the problem to solving the secular equation

$$\mathbf{HC} = \mathbf{SC}\epsilon \tag{2}$$

where **H** is the Hamiltonian matrix over atomic orbitals, **C** is the coefficient matrix of the MO, and **S** is the overlap matrix of the atomic orbitals. The diagonal elements of **H** are usually taken as valence shell ionization energies (VSIE). For the off-diagonal elements two major forms have been used.[3] One, the Wolfsberg–Helmholtz form

$$H_{ij} = kS_{ij}(H_{ii} + H_{jj})/2 \tag{3}$$

where k is a parameter, has been used extensively in transition-metal chemistry. Two, the Hoffmann form

$$H_{ij} = S_{ij}\beta \tag{4}$$

where β is a parameter, has found more applications in organic and main-group chemistry. Several modifications of these forms have been suggested, including different k's or β's for different types of bonds,[3] a product form of eq 3, and Cusachs' suggestion that $k = (2 - |S_{ij}|)$.[9] All of these forms suffer from the fact that the MO coefficients are not independent of the energy scale. That is, if a value Z is added to all H_{ii} terms, only for $k = 1$ in eq 3 will the molecular orbitals remain unaltered. For a systematic examination of the parameters it would be convenient to have a form for which the final MO coefficients (**C** in eq 2) depend only on the relative energy difference between diagonal terms (H_{ii}) and not on their absolute magnitude. The simplest form of the off-diagonal terms, which has this property and a free parameter (K), is

$$H_{ij} = S_{ij}(H_{ii} + H_{jj})/2 \; - S_{ij}K \tag{5}$$

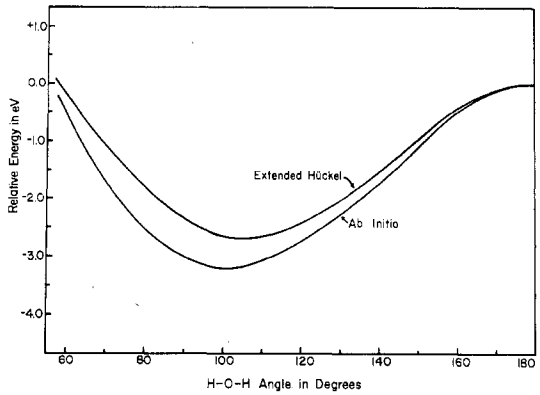

Figure 1. Comparison of ab initio and extended Hückel potential energy curves for H_2O.

To show that this form is capable of reasonable predictions of the geometry, we calculated an ab initio Hartree–Fock–Roothaan (HFR) potential energy curve for the angle in H_2O (R = 1.81 au) using the standard basis functions suggested by Pople.[10] For the EH (extended Hückel) calculation we used the same basis for the calculation of **S** and took the diagonal H_{ii} terms from the diagonal Fock matrix elements (eV) (O 2s = −34, O 2p = −10, H 1s = −16). K was taken as −18 eV, a value which reproduces the O 2s–H 1s off-diagonal Fock matrix element. The results of these two calculations are shown in Figure 1. It is clearly evident that this form of the off-diagonal matrix elements and our method of choosing parameters from the ab initio calculation yield very good agreement between ab initio HFR and EH calculations. This result is in contrast to previous comparisons of HFR and EH calculations, in which the standard EH parameters were used.[4] The initial parameters for all calculations in this work were chosen in an analogous manner from ab initio calculations near the equilibrium geometry and are listed in the Appendix.

The total energy in EHT is usually expressed as

$$E = \sum_i n_i \epsilon_i \tag{6}$$

where n_i is the number of electrons in the ith MO and ϵ_i is its eigenvalue. It is usually assumed that there is an effective cancellation between the electronic Coulomb terms, which are not explicitly included in EHT, and the nuclear repulsions. Thus, we can analyze the total energy equation (6) using Walsh diagrams where the Walsh orbital energies are simply the EHT eigenvalues. In our previous work we found that the major effect of the Pauli repulsions manifests itself in the orthogonality requirements of the localized orbitals. Within the context of EHT we can examine the effect of removing the Pauli repulsions by neglecting the overlap matrix, **S**, in the solution of eq 2. We will often refer to this situation as the nonorthogonal case, but orbitals which belong to different irreducible representations remain orthogonal.

The total energy can also be expressed as

$$E = \sum_a \sum_b D_{ab} H_{ab} \tag{7}$$

where **H** is the Hamiltonian matrix and **D** the density matrix

$$D_{ab} = \sum_i n_i C_{ia} C_{ib} \tag{8}$$

If we now replace the off-diagonal terms of H in eq 7 with eq 5 the total energy reduces to

$$E = \sum_a P_a H_{aa} - K(N - \sum_a D_{aa}) \tag{9}$$

where P_a is the Mulliken gross population ($P_a = \sum_b D_{ab} S_{ab}$) in atomic orbital X_a,[11] H_{aa} is its effective VSIE, and N is the total number of valence electrons. The first term in eq 9 can

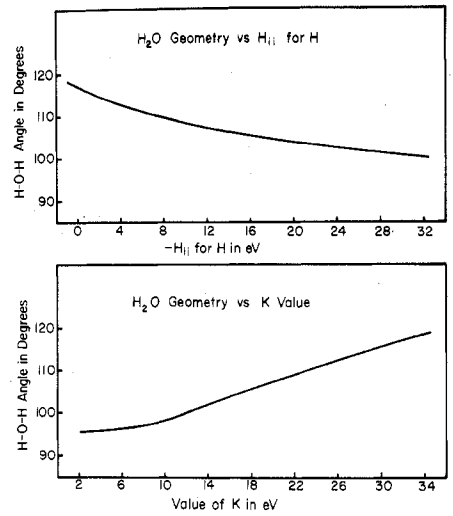

Figure 2. Comparison of the dependence of the H_2O angle on the electronegativity of the H (upper curve) and on the value of the EH parameter K (lower curve).

be identified with the quasiclassical contribution to the energy and the second term with the interference energy.[8] Although the other forms of EHT, eq 3 and 4, can be cast into a form corresponding to eq 9, our form, eq 5, is unique in having an interference term which depends only on K. The quasiclassical term represents the energy contributions due to the effective occupation of various atomic orbitals (the largest contribution arises from the diagonal, $D_{aa}H_{aa}$, terms of eq 7), while the interference term represents the nonclassical contributions to the energy and includes both constructive interference of bond formation and the destructive interference of Pauli repulsions.

Results and Discussion

Detailed Analysis of H_2O. We will first present a detailed analysis of the H_2O molecule and then present our results on other systems in brief. Water was chosen as an example for several reasons. It has, according to VSEPR, lone pair–lone pair, lone pair–bond pair, and bond pair–bond pair repulsions, it is a simple two-coordinate molecule (only one angle need be considered), and it has been subjected to several ab initio studies including our previous work. The geometry of an AH_n molecule within our EHT depends on four things: (1) the basis set chosen for the calculation of **S**, (2) the relative electronegativity of A compared to H, i.e., the relative energy separation between their diagonal terms, (3) the value of K in the expression for the off-diagonal term, eq 5, and (4) the relative energy separation of the np from the ns orbitals of A.

We have examined several basis sets including best atom, multi-ζ Hartree–Fock–Roothaan, and the standard molecular basis of Pople. Although the quantitative results depend on the basis, the qualitative trends we will be discussing do not. The dependence of the geometry of H_2O on the value of H_{ii} for hydrogen and on K is shown in Figure 2. From eq 9 one expects that as K increases the interference term will increase and our results show that the bond angle increases. This result gives us our first hint that the major Pauli repulsions are between bond pairs. The dependence of the geometry on the H_{ii} term for hydrogen is not unexpected. As the H atom becomes more electronegative the bond angle decreases. However, analysis of the energy using eq 9 suggests that there is both a quasiclassical and interference contribution to the decrease in angle so that the decrease in angle is not due solely to a reduction in the Pauli repulsions as suggested by VSEPR. Figure 3 shows a plot of the quasiclassical energy and interference energy for the H_2O parameters given earlier. The geometry is a balance between these two contributions; the

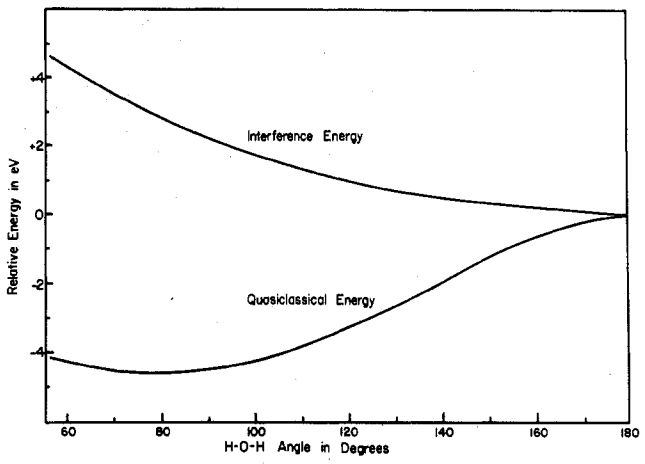

Figure 3. Contributions of the quasiclassical and interference terms to the total energy of H_2O.

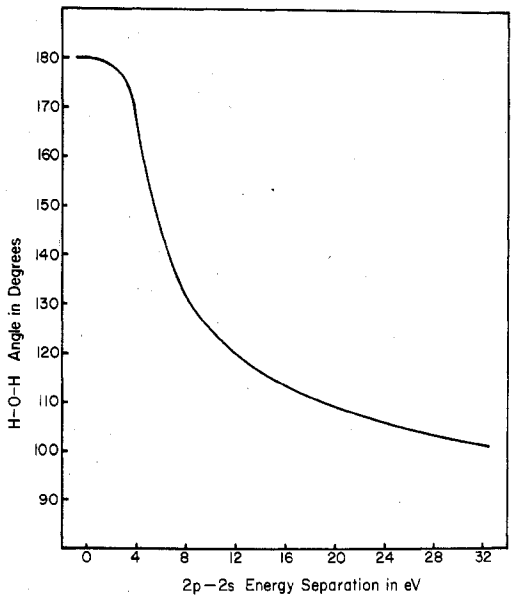

Figure 4. Dependence of the H_2O angle on the relative 2p–2s energy separation of oxygen (same scale as Figure 2).

quasiclassical contribution favors bending, while the interference term favors a linear molecule. As we have pointed out previously the effect of Pauli repulsions is manifest totally in the interference term and would favor a linear structure for water. Thus, if the Pauli repulsions dominated the geometry, a linear molecule would result—not a bent one as suggested by VSEPR. The driving force for bending comes from the quasiclassical term. Because the 2s orbital is lower in energy than the 2p, the quasiclassical contribution will attempt to maximize the occupation of the 2s orbital by bending the molecule and placing more 2s character into the lone pair. We had arrived at this conclusion previously in our ab initio studies of the H_2O geometry.

If our conclusions are correct, the relative 2p–2s energy separation, the last of the four factors which control the EHT results, should be critical for the geometry. In Figure 4 we have plotted the geometry against the relative 2p–2s energy separation. This figure, which has the same scale as Figure 2, shows that of all the factors on which the EHT results depend, the most critical is this energy separation. In order to maintain constant overall electronegativity for the oxygen during this change, we have kept the trace of the oxygen diagonal terms constant. This results in nearly constant hydrogen charges, and the results in Figure 4 are not prejudiced by any contribution from changes in the relative O–H

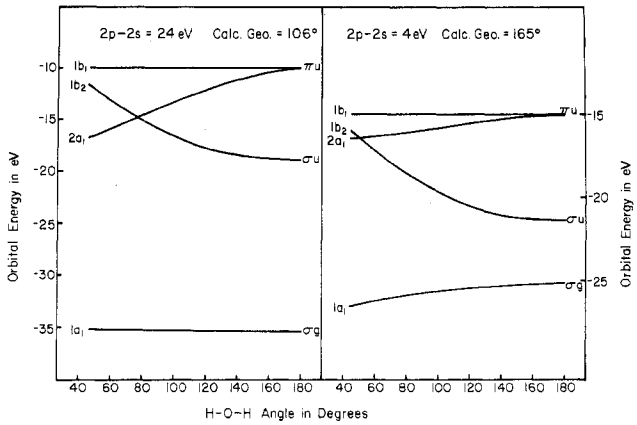

Figure 5. Walsh diagrams for H_2O with different 2p–2s energy separations.

electronegativities. At a 2p–2s energy separation of about 25 eV we obtain an angle of 104°. As this energy separation is increased, we observed a decrease in the angle; however, the decrease is being resisted by the Pauli repulsions between the bond pairs and the angle appears to asymptotically approach 95°. However, as the energy separation is decreased the angle opens up dramatically to 180° without meeting any resistance from the lone pairs. Thus, at a 2p–2s energy separation of 0.0 eV water is a linear molecule with two lone pairs in pure 2p orbitals and two bond pairs in "sp" hybrids. The stereochemical activity of the lone pairs has been eliminated by decreasing the 2p–2s energy separation. Thus, their stereochemical activity really arises from the stereochemical activity of the 2s orbital which, if it is lower in energy than the 2p, would prefer to remain as a lone pair. This result gives further support to our previous contention that Pauli repulsions involving lone pairs are not the primary reason H_2O has an angle less than tetrahedral.

The Walsh diagrams, Figure 5, for two different 2p–2s energy separations, one where the minimum energy angle is 106° and one where it is 165°, provide a clue to how this separation controls the energy. As the 2p–2s energy separation is decreased the curvature of the orbitals on the Walsh diagram generally decrease (note scale difference). For H_2O the curvature of the a_1 orbitals, which favor a bent structure, has decreased more than the curvature of the b_2 orbital, which favors a linear structure. Thus, the 2p–2s energy separation has a controlling influence on the curvature of the levels in a Walsh diagram.

If one neglects the overlap matrix in the solution to eq 2, one removes the Pauli repulsions. In H_2O the angle drops sharply toward 90° for all energy separations greater than zero. This behavior again suggests that the major Pauli repulsions are between bond pairs. The effect of changes in the 2p–2s energy separation can also be analyzed with eq 9. As the 2p–2s energy separation decreases, the quasiclassical contribution to the energy change on bending decreases as one would expect since it represents the energy due to the partitioning of the electron density between the 2s and 2p orbitals. The interference term, however, remains essentially unchanged and represents the energy from bond formation and Pauli repulsions. Thus, at some point the interference term will dominate the total energy and a linear molecule will result. Again, this analysis supports our conclusions that the only important Pauli repulsions in H_2O are between bond pairs.

In the remainder of this paper we will discuss in somewhat less detail our results for other AH_n molecules. The effect of the parameters K and H_{ii} for the ligand H are similar for all the molecules studied. An increase in K or an increase in the H_{ii} for the ligand always favors the most symmetric distribution of ligands. However, the effect of the *n*p–*n*s energy separation on the geometry depends on the total number of valence electrons.

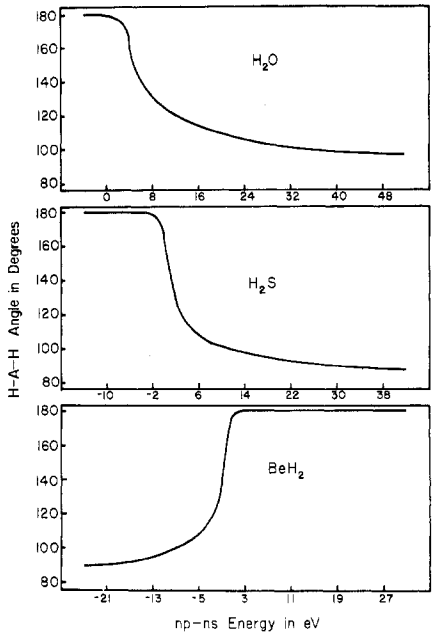

Figure 6. Dependence of the H–A–H angle on the *n*p–*n*s energy separation for H_2O, H_2S, and BeH_2.

AH_2 Systems. The effect of the *n*p–*n*s energy separation on several AH_2 systems is shown in Figure 6. For BeH_2 with two pairs of electrons in the valence shell a linear molecule is found for all 2p–2s separations greater than zero. In this case both the quasiclassical and interference terms favor a linear system. The reason for the change in the effect of the quasiclassical term arises because with only two pairs of electrons the maximum 2s occupation would occur at 180° where the unfilled orbitals on Be are pure 2p. Bending the molecule will force electron density out of the lower energy 2s and raise the quasiclassical contribution to the energy. However, when the 2p–2s energy separation is less than zero, it becomes energetically favorable to depopulate the 2s and populate the 2p, and BeH_2 bends sharply. Within the assumptions of VSEPR there is no way to account for this behavior because VSEPR fails to take account of the energy differences between the 2s and 2p. However, the results can be rationalized within the hybrid orbital approach. Thus, when the 2s is lower in energy than the 2p, the bonding hybrids will contain the maximum amount of 2s, i.e., "sp" hybrids (180°); when the 2p is lower in energy, the bonding hybrids will contain the maximum amount of 2p, i.e., "p^2" hybrids (90°).

The Walsh diagrams of BeH_2 show behavior similar to that of the two lowest orbitals of Figure 5 except that the curvature of the $1a_1$ is larger. As the 2s–2p separation decreases, the curvature of the $1a_1$ orbital increases, and, finally, for separations less than zero its downward curvature, toward smaller angles, is greater than the upward curvature of the $2b_2$ and a bent structure results. BeH_2 is probably linear; our major point is that it is the 2p–2s energy separation which provides much of the driving force, and it is conceivable that for elements early in the periodic table, where the *n*p–*n*s separation is least, other factors might cause bending under favorable circumstances. From our results the most favorable conditions for a bent system with two valence pairs would be a large group 2 central atom to reduce the effect of the interference term and an electronegative ligand to reduce both the quasiclassical and interference terms. Experimentally, the group 2 fluorides most closely meet this criterion and it is found that SrF_2 and BaF_2 are bent.

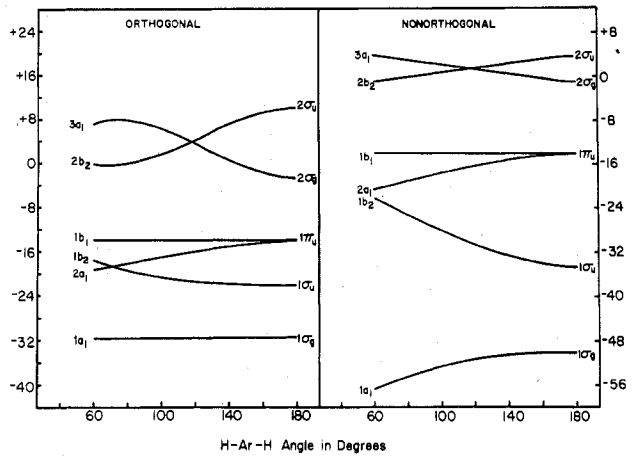

Figure 7. Walsh diagrams for ArH_2 with Pauli repulsions (orthogonal) and without Pauli repulsions (nonorthogonal).

In our preceding discussion we have shown that the geometry of H_2O also depends critically on the 2p–2s energy separation but has behavior opposite that of BeH_2. Thus, for large 2p–2s energy separation one finds a strongly bent geometry, but as 2p–2s separation approaches zero, the geometry becomes linear (see Figure 6). In this case, the quasiclassical and interference terms act in opposing directions. In Figure 6 we also show the dependence of the angle in H_2S on the 3p–3s energy separation. In general the behavior is quite similar to that of H_2O. There are, however, several important differences. For a given value of the energy separation the bond angle is much smaller in H_2S than in H_2O. For large energy separation the bond angle in H_2S asymptotically approaches a smaller angle. As the energy separation decreases, the angle remains smaller than in H_2O until the point where it becomes more favorable to have lone pairs in the p orbitals where the angle increases more abruptly. Taken together, these results suggest that the effect of Pauli repulsions between bond pairs is considerably reduced in the case of H_2S, and, thus, the desire to keep the 3s fully occupied can more easily be satisfied and the bond angle is closer to 90°. This analysis provides a simple reason for the dramatic decrease in angle observed when going from a first- to a second-row hydride. This observed decrease in angle cannot be explained within the framework of VSEPR. A rationale for the linear nature of Li_2O is also provided by these concepts. The very electropositive lithium will provide a higher energy diagonal term (H_{ii}) and increase the occupation of the oxygen orbitals such that the effect of the quasiclassical term is reduced and the interference term dominates the geometry.

Although ArH_2 does not exist, it forms a close analogy to XeF_2, especially, since we have made the H's somewhat more electronegative (decreased H_{ii} for H by 2 eV). The effect of the 3p–3s energy separation on the geometry of ArH_2 is quite different. For large separations ArH_2 is predicted to be linear; as the separation decreases, the molecule remains linear until a change in electronic configuration occurs as the separation approaches zero. The Walsh diagrams, Figure 7, show that for the linear case the highest filled MO is the $2\sigma_g$ ($3a_1$) which essentially fills the 3s orbital making it a lone pair for all angles and causing the loss of its stereochemical activity, i.e., the quasiclassical term no longer favors bending and the molecule opens to a linear geometry. An analysis in terms of eq 9 suggests that the geometry is dominated by the interference energy. When the 3p–3s separation is less than zero, the lowest energy configuration has the $2b_2$ ($2\sigma_u$) filled instead and the total energy favors a bent geometry. Thus, the stereochemical activity of the 3s orbital is relegated to determining the ground-state electronic configuration.

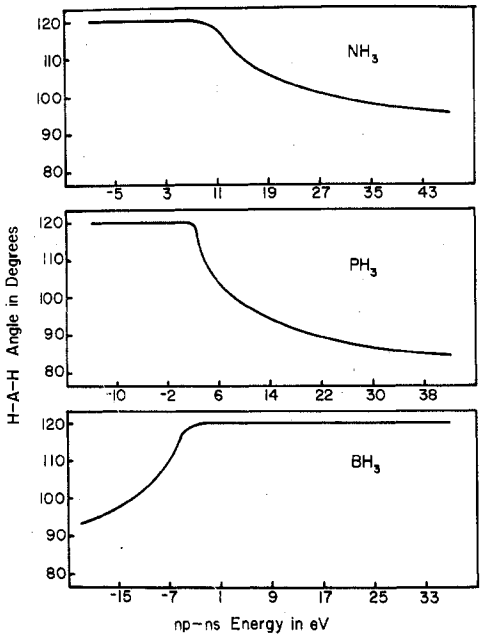

Figure 8. Dependence of the internal AH_3 angle on the *n*p–*n*s energy separation for NH_3, PH_3, and BH_3.

The effect of the Pauli repulsions can be assessed from the comparison in Figure 7 which shows the Walsh diagram both with and without Pauli repulsions. Without Pauli repulsions (nonorthogonal) the effect of the bonding and antibonding a_1 orbitals ($2a_1$ and $3a_1$) cancel each other, and the barrier to bending arises primarily from the $1b_2$ which loses bonding character on bending. This constructive interference represents an important contribution to the barrier, which suggests that "three-center, four-electron" bonds have a natural rigidity apart from any Pauli repulsion. When the Pauli repulsions are included, more of the curvature appears in the upper orbitals and the rise in the $3a_1$ favors a linear configuration. The Pauli repulsions double the value of the barrier to bending (180° → 175°). The change in the curvature of the levels between Figure 7 reflects an important effect of the Pauli principle in that it makes the energy of the HOMO a primary contribution to the geometry and will be a key ingredient of any frontier orbital approach. As has been recently pointed out, many of the failures of CNDO can be attributed to the neglect of the overlap in solving eq 2,[13] i.e., a failure to properly include the Pauli repulsions.

AH_3 Systems. The effect of the *n*p–*n*s energy separation on AH_3 systems is shown in Figure 8. The results for BH_3 are analogous to those of BeH_2. For large 2p–2s separations it is energetically more favorable to have the empty orbital on B as a 2p and use the 2s in bonding, which results in a planar structure. When population of the 2p becomes more favorable, the system goes to a pyramidal geometry in an attempt to empty the 2s orbital. This bending is of course resisted by the Pauli repulsion between bond pairs.

NH_3 and PH_3 show behavior similar to that of H_2O and H_2S. Here the single lone pair would prefer to occupy the *n*s orbital as long as it is lower in energy than the *n*p, which results in a pyramidal geometry. However, if the *n*p orbital becomes energetically favored, the system becomes planar with the lone pair in the *n*p orbital. In this process of opening up the bond angle there is no resistance due to any lone pair–bond pair Pauli repulsions. The larger angle observed for NH_3 compared to H_2O arises simply from an increase in the Pauli repulsions between bond pairs due to the fact that there are three instead of two bond pairs. The decrease in angle in PH_3 (compared to NH_3) is apparent in Figure 8 and arises again from the larger size of the central atom, which decreases the importance

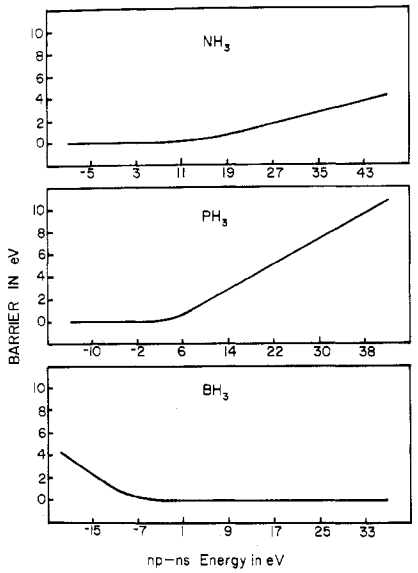

Figure 9. Dependence of the barrier to inversion of NH_3, PH_3, and BH_3 on the *n*p–*n*s energy separation.

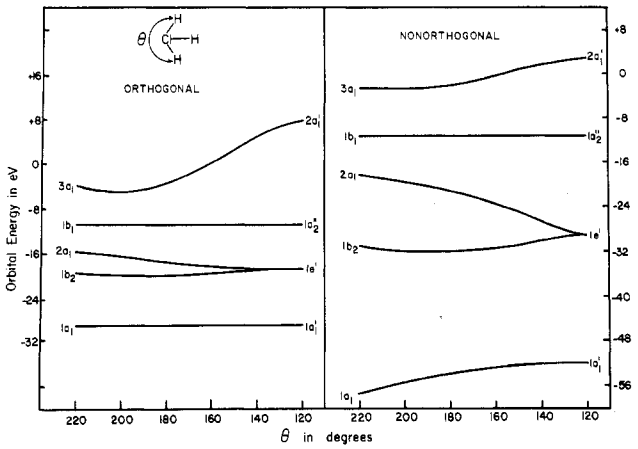

Figure 10. Walsh diagrams for ClH_3 with and without Pauli repulsions.

of the interference term (Pauli repulsion) so that quasiclassical term now becomes more effective in reducing the bond angle.

The barriers to inversion of NH_3 and PH_3 as a function of *n*p–*n*s separation are shown in Figure 9. As the *n*p–*n*s separation increases, both barriers increase, but the PH_3 barrier increases much more dramatically because the interference term, which favors the planar structure, is not as important in this case. The inversion barriers have recently been discussed by several workers.[14] These workers attribute the larger barrier in PH_3 to the small HOMO–LUMO separation which results in greater stabilization upon bending in PH_3. This separation is controlled by two factors. The first is the *n*p–*n*s energy separation. As this separation increases, the HOMO–LUMO separation decreases and the barrier increases as shown in Figure 9. The second involves the relative size of the two central atoms. The energy of the LUMO, which is antibonding between the *n*s and the a_1 combination of the hydrogens, is strongly influenced by the H–H interactions. As these are larger in NH_3 than PH_3, the interaction is stronger with the N 2s and results in a higher energy LUMO. It is this last effect which gives rise to the larger experimental barriers since the *n*p–*n*s energy separation will be larger for NH_3.

Figure 10 displays the Walsh diagrams for ClH_3 in the C_{2v} point group both with and without Pauli repulsions. The molecule will be T shaped in both cases. As in ArH_2 the

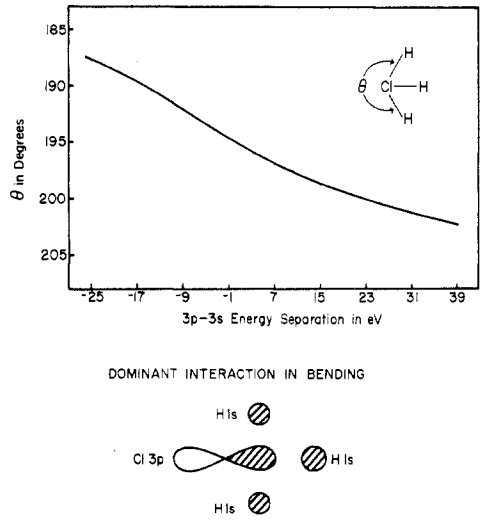

Figure 11. Dependence of the H–Cl–H angle in ClH_3 on the 3p–3s energy separation and the dominant interaction responsible for this trend.

addition of the **S** matrix forces much more curvature into the upper levels and they will dominate the bond angle. In the nonorthogonal case the bending back toward the unique H is due primarily to a gain in the bonding of the symmetric combination of H's with the 3p orbital which is involved in the bond to the unique H ($1a_1$ and $3a_1$ MO). The $2a_1$ favors a C_{3v} structure, while the $1b_2$, which represents the three-center bonding orbital, favors a linear 3c-4e system. Orthogonality increases the degree of bending toward the unique H, and analysis of the interference term suggests that this is a magnification of the same interaction. Thus, the bending of the "axial" hydrogens in ClH_3 toward the unique hydrogen is primarily controlled by their interaction with the 3p orbital that lies along the unique Cl–H axis (see Figure 11). The 3p–3s energy separation has an important contribution to the bond angle. First, it again controls the electronic configuration which in turn controls the geometry. However, even for smaller variations in the 3p–3s energy separation, where the T shape is always the minimum energy, the separation has an important effect on the geometry. Figure 11 shows that, as the separation increases and the 3s orbital becomes pure lone pair, the system bends back more toward the unique hydrogen. Thus, as the directional properties of the lone pair decrease, the system bends further away from it, a result at variance with VSEPR. Analysis of this result suggests that the primary reason for bending is the interaction with the 3p orbital along the unique axis and not with the lone pair (see Figure 11). It is not important how this 3p orbital is partitioned between the Cl–H bond and the lone pair, but its energy relative to the a_1 combination of "axial" hydrogens is of primary importance. Thus, the electron-rich three-center, four-electron bond can lower its energy by delocalizing into the electron-poor two-center, two-electron bond.

AH_4 Systems. Methane and silane remain tetrahedral for all parameters tried both with and without orthogonality. This result is to be expected since there are neither lone pairs nor empty orbitals on the central atom. Our analysis indicates that the geometry is dominated by interference terms.

However, when two more electrons are added to form SH_4, we find that the geometry is extremely sensitive to the 3p–3s energy separation. In Figure 12 we show a partial energy surface for both small and large 3p–3s energy separations in the same electronic configuration. For a small separation the geometry is planar D_{4h} and only for a large separation do we find the expected pyramidal shape. Figure 12 shows that the C_{4v} and C_{2v} geometries are very close in energy. This is not

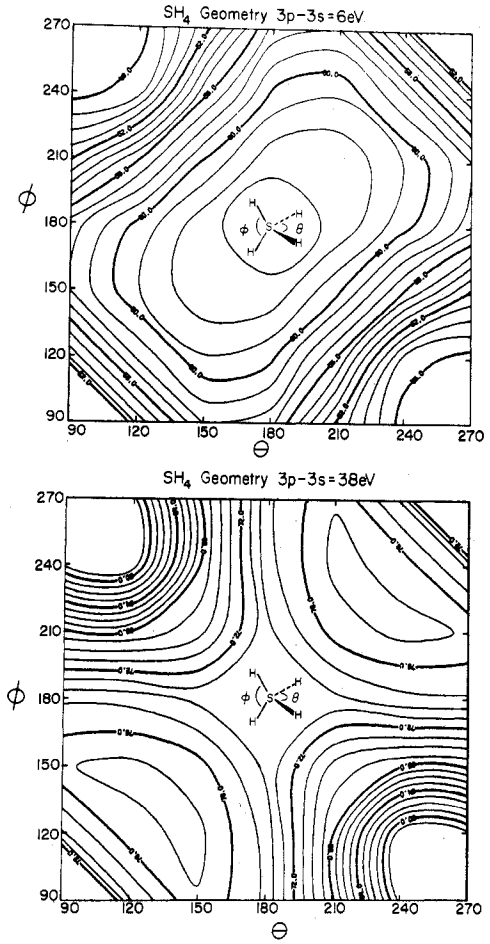

Figure 12. Potential energy surfaces of SH_4 for two different 3p–3s energy separations (contours are negative).

unexpected since previous ab initio calculations have shown that the geometries of species isoelectronic with SF_4 and SH_4 are extremely sensitive to the choice of basis.[15] Hoffmann has also noted the strong dependence of the geometry on parameter choice in sulfuranes.[16] For small energy separations it is energetically more favorable to put the lone pair in a pure 3p orbital and a planar structure results. As the 3s becomes sufficiently more stable than the 3p, the lone pair changes character to a 3s and a bent geometry results. Of all main-group hypervalent molecules known, molecules isoelectronic with SH_4 are unique in that only these molecules have more than one "normal" covalent bond and at least one lone pair. It is this fact which makes their geometry so sensitive to the 3p–3s separation. Analysis of the energy with eq 9 shows that the interference term always favors the D_{4h} geometry, and it is the quasiclassical term which accounts for the deformation to a pyramidal geometry (i.e., lower energy 3s orbital). This conclusion is also supported by the solution of eq 2 without the overlap matrix (without Pauli repulsions). Again, the system is planar until the 3s orbital is sufficiently lower in energy to cause bending to the pyramidal geometry. Thus, the Pauli repulsions in SH_4 always favor a D_{4h} geometry and bending away from this geometry is only favored if the 3s is low enough in energy that increasing its occupation will lower the total energy.

In ArH_4 the geometry is planar, D_{4h}, for all large 3s–3p energy separations, but for separations less than about 10 eV there is a change in configuration as in ArH_2 and the system distorts to a pyramidal structure. Thus, the 3p–3s energy separation controls the geometry through a determination of the energy level ordering. In the planar geometry the 3s orbital is fully occupied and the molecule is well described as having

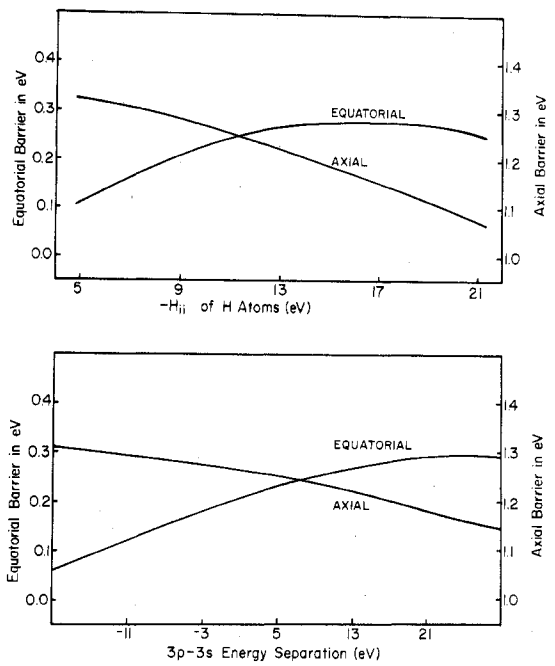

Figure 13. Dependence of the barriers in PH_5 for converting a trigonal-bipyramidal geometry to a square-pyramidal geometry on the electronegativity of the ligands and on the 3p–3s energy separation.

two three-center, four-electron bonds. As with ArH_2 there is both a quasiclassical and interference contribution to the barrier for bending the molecule out of the D_{4h} geometry. In this case the addition of orthogonality increases the barrier nearly threefold. Thus, the molecule would be planar in the absence of Pauli repulsions but not nearly as rigid.

AH_5 Systems. Several workers[17] have recently studied AX_5 systems especially with regard to their fluxional character. PH_5 shows a regular trigonal-bipyramidal structure for a variety of parameters. An increase in K increases the barrier to bending toward a square pyramid for both the axial and equatorial ligands. As shown in Figure 13, both the electronegativity of the ligands (H_{ii}) and 3p–3s energy separation are equally important in determining the barrier to distortion from a trigonal bipyramid to a square pyramid. An increase in electronegativity of the ligands or in the 3p–3s energy separation increases the equatorial barrier while decreasing the axial barrier. This behavior is consistent with the axial system being mainly a three-center, four-electron bond and the equatorial system being mainly two-center, two-electron bonds. Removal of the Pauli repulsions lowers the axial barrier and raises the equatorial barrier as one would expect for this description of the bonding.

The bonding in ClH_5 is quite similar to that in ClH_3 but with an additional three-center, four-electron bond. ClH_5 exhibits C_{4v} geometry for a variety of parameters, although another geometry might occur if we changed the 3p–3s separation enough to cause a change in the electronic configuration. As the 3p–3s separation is increased, the 3s becomes more lone pair like and the equatorial hydrogens bend back more toward the unique axial hydrogen. A similar situation was observed in ClH_3 and can be attributed to the interaction of the symmetric equatorial combination of hydrogens with the 3p orbital whose phase is determined by the unique H.

AH_6 Systems. SH_6 shows an octahedral geometry for a wide variety of parameters. The barrier to bending away from O_h symmetry appears to be rather independent of the 3p–3s separation and the electronegativity of the H but depends strongly on the value of K. Thus, like that of SiH_4 and to a lesser degree PH_5, the geometry of SH_6 is dominated by the

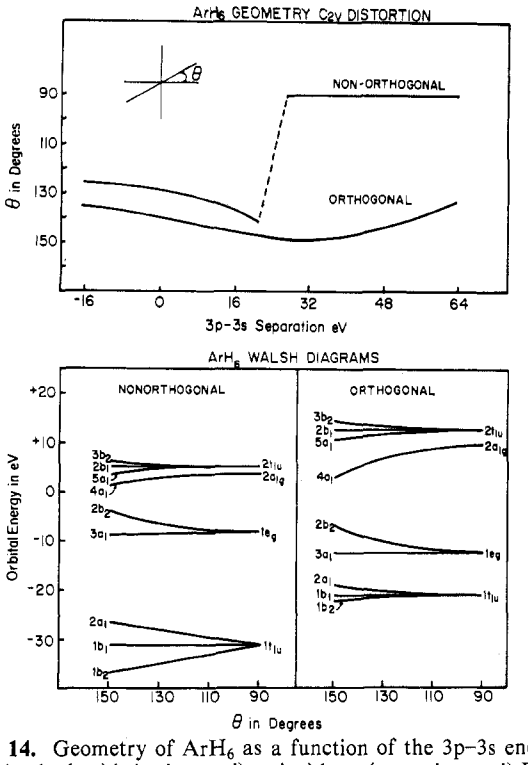

Figure 14. Geometry of ArH_6 as a function of the 3p–3s energy separation both with (orthogonal) and without (nonorthogonal) Pauli repulsions. Walsh diagrams for ArH_6 both with and without Pauli repulsions.

interference terms and Pauli repulsions between bond pairs.

In ArH_6 which has an additional electron pair the distortion away from O_h is calculated to be substantial in the EH method.[18] Increasing K decreases the distortion, while increasing the electronegativity of the ligands increases the distortion. The distortion also has a weak dependence on the 3p–3s separation; as shown in Figure 14, it is largest for an intermediate value and decreases for either smaller or larger separations. This is to be expected if one views the distortion as a second-order Jahn–Teller effect since the 3p–3s separation will control the HOMO–LUMO energy separation. Except for very large 3p–3s separations the C_{2v} distortion appears to be lower in energy than the C_{3v} distortion, but this may be an artifact of the EHT. A comparison of the Walsh diagrams for the orthogonal and nonorthogonal cases is also shown in Figure 14. For the nonorthogonal case (without Pauli repulsions) the geometry is octahedral until the 3p–3s separation is small enough to cause the $2t_{1u}$ orbitals to be occupied instead of the a_{1g}. When the Pauli repulsions are included, the downward curvature of the highest a_{1g} increases leading to a distorted geometry for all separations. Thus, the Pauli repulsions are intimately connected with the distortion of the molecule and with the mechanism of the second-order Jahn–Teller effect. An analysis of the energy terms in eq 9 shows that for small 3p–3s separations both the quasiclassical and interference terms favor distortions from O_h, but for larger separations the quasiclassical terms favor octahedral while the interference terms favor a distorted geometry.

Effect of d Orbitals. We have also investigated the effect of the addition of 3d orbitals on the geometry of the hypervalent molecules. We chose the same exponent for the 3d as for the 3s and 3p, and we examined the effect of making the 3d more important by lowering its H_{ii} terms while raising the H_{ii} of the 3s and 3p such that the central atom had approximately the same electronegativity. For molecules with a high symmetry geometry such as ArH_2, SiH_4, ArH_4, PH_5, and SH_6, as the 3d orbitals became more important, the barriers to distortions in all cases became smaller. Thus, the 3d orbitals decreased the rigidity of the molecules. For the molecules ClH_3, SH_4, ClH_5, and ArH_6, the addition of 3d orbitals reduced the distortions; thus, the "axial" H–Cl–H system in ClH_3 came closer to 180° as the importance of the 3d orbitals was increased. Similar effects have previously been observed in the geometry of hypervalent molecules with ab initio calculations.[15] As in that work we may conclude that the d orbitals are not critical for the gross geometry but will be important for the quantitative prediction of bond angles and barriers.

Table I. Extended Hückel Parameters (eV) and Bond Distances (Å)

atom A	*n*s A	*n*p A	1s H	*K*	A-H
Be	−7.0	−4.0	−7.5	+12.0	1.34
B	−13.0	−4.0	−10.0	+14.0	1.19
C	−22.0	−8.0	−13.0	+14.0	1.09
N	−28.0	−9.0	−15.0	+15.0	1.01
O	−34.0	−10.0	−16.0	+18.0	0.96
Si	−15.0	−3.0	−10.0	+13.0	1.48
P	−19.5	−5.5	−11.0[a]	+14.0	1.43
S	−23.0	−9.0	−13.0[a]	+15.0	1.34
Cl	−26.5	−11.5	−15.0[a]	+15.0	1.27
Ar	−30.0	−14.0	−17.0[a]	+15.0	1.20

[a] For hypervalent cases these values were more negative by 2.0 eV.

Conclusion

Although this study was based on the very approximate EHT, we believe that the gross features displayed by this method will also play an important role in the geometries regardless of the theoretical approach used. Our results suggest that the relative energy separation of the *n*s to *n*p atomic orbitals on the central atom plays a key role in determining the bond angles of main group molecules. It determines the angle between two-electron, two-center bonds by controlling the curvature of the energy levels. In hypervalent molecules this separation controls the electronic configuration and the degree to which three-center, four-electron bonds are bent toward the normal covalent bonds. This energy separation has played an important role in the traditional concepts of valence bond theory,[19] but its importance is neglected in VSEPR and not always obvious in MO treatments. In normal covalent molecules the only important Pauli repulsions are those between bond pairs. In hypervalent molecules Pauli effects also contribute to the geometry of three-center, four-electron bonds. However, the bending away from the lone pair does not appear to be caused by lone pair repulsions but by bond pair effects, i.e., the lower total energy arising from the delocalization of the "electron rich" three-center, four-electron bond into the "electron poor" two-center, two-electron bond. Pauli effects also play a key role in the distortions of XeF_6 from O_h symmetry.

Acknowledgment. Acknowledgment is made to the donors of the Petroleum Research Fund, administered by the American Chemical Society, to the Robert A. Welch Foundation (Grant A-648), and to the National Science Foundation (Grant CHE77-07825) for support of this work.

Appendix

The bond distances and the EH parameters, which were extracted from ab initio calculations and used as our starting points, are listed in Table I. Since we have been interested in how the bond angles depend on variations of these parameters, they have not been optimized to reproduce the geometry. Although our experience indicates they will yield reasonable bond angles in most cases, they should be used with caution.

Registry No. BeH_2, 7787-52-2; BH_3, 13283-31-3; CH_4, 74-82-8; NH_3, 7664-41-7; H_2O, 7732-18-5; SiH_4, 7803-62-5; PH_3, 7803-51-2; PH_5, 13769-19-2; SH_2, 7783-06-4; SH_4, 51621-86-4; SH_6, 51715-67-4; ClH_3, 66653-01-8; ClH_5, 66653-00-7; ArH_6, 66674-95-1.

References and Notes

(1) M. B. Hall, *J. Am. Chem. Soc.*, to be submitted for publication.
(2) R. J. Gillespie and R. S. Nyholm, *Q. Rev., Chem. Soc.*, **11**, 339 (1957); R. J. Gillespie, *Angew. Chem., Int. Ed. Engl.*, **6**, 819 (1967).
(3) M. Wolfsberg and L. Helmholz, *J. Chem. Phys.*, **20**, 837 (1952); R. Hoffmann and W. N. Lipscomb, *ibid*, **36**, 2179, 3489 (1962); **37**, 2873 (1962).
(4) L. C. Allen and J. D. Russell, *J. Chem. Phys.*, **46**, 1029 (1967); L. C. Allen, *Theor. Chim. Acta*, **24**, 177 (1972).
(5) B. M. Gimarc, *J. Am. Chem. Soc.*, **92**, 266 (1970); **93**, 593, 815 (1971).
(6) L. S. Bartell, *Inorg. Chem.*, **5**, 1635 (1966); *J. Chem. Educ.*, **45**, 754 (1968); L. S. Bartell and V. Plato, *J. Am. Chem. Soc.*, **95**, 3097 (1973).
(7) A. D. Walsh, *J. Chem. Soc.*, 2260, 2266, 2288, 2296, 2301, 2306 (1953).
(8) K. Ruedenberg, *Rev. Mod. Phys.*, **34**, 326 (1962).
(9) C. J. Ballhausen and H. B. Gray, *Inorg. Chem.*, **1**, 111 (1962); L. C. Cusachs, *J. Chem. Phys.*, **43**, S157 (1965).
(10) W. J. Hehre, R. Ditchfield, R. F. Stewart, and J. A. Pople, *J. Chem. Phys.*, **52**, 2769 (1970).
(11) R. S. Mulliken, *J. Chem. Phys.*, **23**, 1833, 1841, 2338, 2343 (1955).
(12) J. P. Lowe, *J. Am. Chem. Soc.*, **96**, 3759 (1974).
(13) A. R. Gregory and M. N. Paddon-Row, *J. Am. Chem. Soc.*, **98**, 7521 (1976); P. Caramella, K. N. Houk, and L. N. Domelsmith, *ibid.*, **99**, 4511 (1977).
(14) C. C. Levin, *J. Am. Chem. Soc.*, **97**, 5649 (1975); W. Cherry and N. Epiotis, *J. Am. Chem. Soc.*, **98**, 1135 (1975).
(15) M. F. Guest, M. B. Hall, and I. H. Hillier, *J. Chem. Soc., Faraday Trans. 2*, 1829 (1973); L. Radom and H. F. Schaefer III, *Aust. J. Chem.*, **28**, 2069 (1975); R. Gleiter and A. Veillard, *Chem. Phys. Lett.*, **37**, 33 (1976); S. R. Ungemach and H. F. Schaefer III, *ibid.*, **38**, 407 (1976).
(16) M. M. L. Chen and R. Hoffmann, *J. Am. Chem. Soc.*, **98**, 1647 (1976).
(17) R. Hoffmann, J. M. Howell, and E. L. Muetterties, *J. Am. Chem. Soc.*, **94**, 3047 (1972); A. Strich and A. Veillard, *ibid.*, **95**, 5574 (1973); A. Rauk, L. C. Allen, and K. Mislow, *ibid.*, **94**, 3035 (1972).
(18) L. S. Bartell and R. M. Gavin, Jr., *J. Chem. Phys.*, **48**, 2466 (1968).
(19) L. Pauling, "The Nature of the Chemical Bond", 3rd ed, Cornell University Press, Ithaca, N.Y., 1960, p 120; C. A. Coulson, "Valence", 2nd ed, Oxford University Press, Oxford, 1961, pp 163, 179, 221.

Contribution from the Department of Chemistry, Texas A&M University, College Station, Texas 77843

Photoelectron Spectra of Substituted Chromium, Molybdenum, and Tungsten Pentacarbonyls. Relative π-Acceptor and σ-Donor Properties of Various Phosphorus Ligands

LINTON W. YARBROUGH, II,[1] and MICHAEL B. HALL*

Received December 29, 1977

The UV photoelectron spectra (PES) of the transition-metal complexes $LM(CO)_5$, where M = Cr, Mo, or W and L = PEt_3, PMe_3, $P(NMe_2)_3$, $P(OEt)_3$, $P(OMe)_3$, or PF_3, are reported and compared with the PES of the uncoordinated ligands. Particular emphasis is placed on the assignment of the metal d orbital band components, the M–P bond, and the P nonbonding pair in the free ligand. The ability of the ligands to split the t_{2g} orbitals of the parent hexacarbonyl into the e and b_2 components falls in the order $PEt_3 \sim PMe_3 > P(NMe_2)_3 > P(OEt)_3 \sim P(OMe)_3 > PF_3$ and follows the inverted order of π-acceptor ability of these ligands. The σ-donor ability is reflected in the ionization potential (IP) of the M–P bond and falls in the order $PEt_3 \sim PMe_3 > P(OEt)_3 \sim P(OMe)_3 > P(NMe_2)_3 > PF_3$. Comparisons of the free and complexed ligands allow us to make definitive assignments of the PES bands of the free ligands, assignments about which there has recently been considerable controversy. The spin–orbit coupling (SOC) parameters of the W complexes remain unexpectedly constant through this series of ligands rather than decreasing as their π-acceptor ability increases. We attribute this constancy to the ability of CO to release electron density to the metal, thus, compensating for loss of density as the π-acceptor ability of L increases. Therefore, the total delocalization of the metal remains constant. The σ/π parameters derived from the PES are also compared with those from CO force constants. Fenske–Hall molecular orbital (MO) calculations were done on the Cr complexes of PMe_3, $P(NMe_2)_3$, $P(OMe)_3$, and PF_3 and the results of these calculations support our assignments.

Introduction

Photoelectron spectroscopy (PES) has proven to be a valuable tool in the elucidation of the electronic structure of molecules.[2] Previous work by M.B.H. has shown the value of comparing the PES of first- and third-row transition-metal complexes.[3] The effect of spin–orbit coupling on the spectra in the case of $XRe(CO)_5$ species provided a definitive assignment and a measure of the total delocalization of the metal d electrons.

In this work we have undertaken a study of the PES of $LM(CO)_5$ systems where M is a group 6B metal (Cr, Mo, or W) and L is a phosphorus ligand (PEt_3, PMe_3, $P(NMe_2)_3$, $P(OEt)_3$, $P(OMe)_3$, or PF_3). Although there have been a number of recent papers dealing with the relative π acceptor and σ donor properties of the phosphine and phosphite ligands in these pentacarbonyls, most of the conclusions about these electronic properties have been based on the measurements of CO stretching frequencies[4] or ^{183}W–^{31}P coupling constants.[4g,5] There have been only a few studies on the electronic structure via more direct measurements such as PES.[6] These PES studies have also been under lower resolution than the results to be reported here.

The relative π-acceptor properties of these ligands should be reflected in the degree to which the t_{2g} of the parent hexacarbonyl is split into an e and b_2. In the case of tungsten the e is further split by the spin–orbit coupling into an e′ and e″ of the double group C_{4v}*.[3] Since the b_2 is also of e″ symmetry under the spin–orbit Hamiltonian, there is some interaction between it and the other e″ component. As we have shown previously,[3] a study of this effect can increase our confidence in a particular assignment and provide us with a measure of the total delocalization of the metal d electrons.

The relative σ-donor strength of ligands should be reflected to a large degree by the ionization potential (IP) of the M–P bonding molecular orbital (MO). The comparison between the free and coordinated ligand spectra also provides a definitive assignment for the P lone pair (donor orbital), since it will be perturbed more severely than the other ligand orbitals on coordination. There has been considerable controversy recently concerning the assignment of several of these ligands,[7] which is resolved by this work.

Experimental and Theoretical Section

Preparation. All solvents were dried over molecular sieves and purged with N_2. Where possible, all materials were handled in an

0020-1669/78/1317-2269$01.00/0